FLORE
Repository istituzionale dell'Università degli Studi di Firenze

Comparative Numerical Study on Left Ventricular Fluid Dynamics after Dilated Cardiomyopathy

(Article begins on next page)

27 April 2024

Comparative numerical study on left ventricular fluid dynamics after dilated cardiomyopathy

Jan O. Mangual [a,*], Elisabeth Kraigher-Krainer [b], Alessio De Luca [c], Loira Toncelli [c], Amil Shah [b], Scott Solomon [b], Giorgio Galanti [c], Federico Domenichini [a], Gianni Pedrizzetti [d,e]

[a] Department of Civil and Environmental Engineering, University of Florence, Italy
[b] Department of Cardiovascular Medicine, Brigham and Women's Hospital, Boston, MA, USA
[c] Sport Medicine Center, University of Florence, Italy
[d] Department of Engineering and Architecture, University of Trieste, Italy
[e] Department of Cardiology, Mount Sinai School of Medicine, New York, NY, USA

ABSTRACT

Introduction: The role of flow on the progression of left ventricular (*LV*) remodeling has been presumed, although measurements are still limited and the intraventricular flow pattern in remodeling hearts has not been evaluated in a clinical setting. Comparative evaluation of intraventricular fluid dynamics is performed here between healthy subjects and dilated cardiomyopathy (*DCM*) patients.
Methods: *LV* fluid dynamics is evaluated in 20 healthy young men and 8 *DCM* patients by combination of 3D echocardiography with direct numerical simulations of the equation governing blood motion. Results are analyzed in terms of quantitative global indicators of flow energetics and blood transit properties that are representative of the qualitative fluid dynamics behaviors.
Results: The flow in *DCM* exhibited qualitative differences due to the weakness of the formed vortices in the large *LV* chamber. *DCM* and healthy subjects show significant volumetric differences; these also reflect inflow properties like the vortex formation time, energy dissipation, and sub-volumes describing flow transit. Proper normalization permitted to define purely fluid dynamics indicators that are not influenced by volumetric measures.
Conclusion: Cardiac fluid mechanics can be evaluated by a combination of imaging and numerical simulation. This pilot study on pathological changes in *LV* blood motion identified intraventricular flow indicators based on pure fluid mechanics that could potentially be integrated with existing indicators of cardiac mechanics in the evaluation of disease progression.

© 2013 Elsevier Ltd. All rights reserved.

1. Introduction

There is an increasing consensus that maladaptive fluid mechanics contributes to cardiac inefficiency and participates in the modulation toward phenotypic patterns of heart failure (*HF*) (Bolger et al., 2007; Pedrizzetti et al., 2010; Sengupta et al., 2012b). *HF* is associated with ventricular remodeling: modification of the *LV*, which progressively alters its function. Studies have reported *HF* in patients with distinct phenotypes exhibiting differences in structure and function (Sengupta and Narula, 2008); modification of the intraventricular flow in remodeled hearts can be presumed theoretically (Baccani et al., 2002) and has been reported in

Cardiac Magnetic Resonance (*CMR*) studies (Carlhäll and Bolger, 2010), although it has not been systematically evaluated in a clinical setting.

The availability of models that can forecast progression/reversal of *LV* remodeling following therapies would be invaluable in overall risk stratification and/or therapeutic intensity. Several pathophysiologic mechanisms have been suggested, nevertheless there is paucity of clinical markers that can characterize a hemodynamic milieu predictive of the risk of cardiac remodeling either following infarction (Nijveldt et al., 2009; Wu et al., 2008) or excessive sport activity (De Luca et al., 2011; Mihl et al., 2008).

The role of flow in cardiac remodeling has been hypothesized (Cimino et al., 2012; Yang et al., 2007) but not clarified. Remodeling refers to changes of ventricular size and shape that result in alteration of the blood motion inside the *LV*. Flow analysis has the potential to represent an early predictor of changes in *LV* function. Nevertheless, the knowledge of intraventricular flow in pathologic

conditions is very limited and clinical references for diagnostic use are missing (Sengupta et al., 2012b).

This work presents a study on the changes in *LV* flow patterns in patients with *DCM* compared to healthy subjects. The fluid dynamics analysis is performed by a combination of 3D echocardiographic imaging with numerical solutions of the equations governing blood motion (Mangual et al., 2012b). The objective was to start building a series of clinical indicators based on fluid-mechanical concepts (Mangual et al., 2012a) and quantify them in extreme cases of healthy and dilates *LVs*. These could provide an initial reference support in the detection of intraventricular flow changes during progressive remodeling.

2. Methods

2.1. Clinical procedure

8 patients diagnosed with *DCM*, with elevated Nt-pro BNP levels (median: 2881.80, IQR: 1648.3 pg/mL), that did not evidence mitral/aortic regurgitation, were enrolled at the Brigham and Women's Hospital (Boston, MA). These patients were compared to a homogeneous group of 20 healthy subjects (19 years old mean age, training 2–3 days/week for 2 h/day) enrolled at the Sport Medicine Center of the University of Florence (Florence, Italy). Enrollment was performed in agreement with the Institutional Review Board; subjects gave their written or oral consent. 2D and 3D transthoracic echocardiography were performed at rest; all subjects were previously selected to exclude those with contradictory characteristics or sub-optimal acquisitions.

2.2. Flow imaging procedure

An echocardiographic 3D full volume image of the left ventricle was recorded on GE (Vivid 7, at Boston), or Philips (IE33, at Florence) machines, at the highest possible frame rate (20–30 Hz). Images were processed by 3D feature tracking (4DLVA 3.0, TomTec Gmbh, Unterschleissheim, Germany) and the endocardial moving surface during one complete heartbeat was exported for the numerical flow analysis for each volunteer. Care was taken to ensure high quality of the 3D results by comparing global longitudinal strain with the value obtained by the multi-plane 2D speckle tracking analysis (2D CPA, TomTec Gmbh, Unterschleissheim, Germany).

Blood flow in the *LV* was not available from direct measurements and was reconstructed by numerical simulations. Blood has known physical properties and its motion obeys the mathematical laws governing the mechanics of fluids: conservation of mass (continuity equation) and conservation of momentum (Navier–Stokes equation) whose solution can be performed by numerical techniques which, when directly solved without approximation (without turbulence models, since approximations related to the discretization of the domain are unavoidable), are called direct numerical simulations (*DNS*). The mean computational resolution used in the simulations was 0.17 cm, chosen after preliminary studies that ensured adequate resolution without affecting the evolution of flow (Mangual et al., 2012a).

DNS can compute the intraventricular blood motion that corresponds to the *LV* moving geometry and properties of the inlet/outlet orifice. Mitral/aortic openings were modeled as orifices with a fixed circular shape and simple open/close behavior. The orifice size was evaluated through pulsed-wave Doppler, taking the *LV* volume rate and transmitral/aortic *PW* Doppler velocity ratio. Although the orifice openings are not exactly circular in shape, care was taken to ensure that the effective orifice area would agree with the obtained transmitral jet velocity from *PW* Doppler. It is evident that the inlet geometry (Lancellotti et al., 2010) and dynamics of the valves (Dimasi et al., 2012) would indeed affect the transmitral velocity and shape of the overall 3D vortex, yet limitations in non invasive imaging did not allow estimating geometrical details of such. Values of the orifice areas are reported in Table 1, which may differ from sizes based on the annulus edges that contain the valvular effective opening. The mean (heartbeat averaged) value of the angle between the mitral and the aortic orifice resulted in $125 \pm 29°$ and $135 \pm 34°$ for the healthy and *DCM* patients, respectively (Veronesi et al., 2009). With this in mind, the work presented herein is aimed as a simple integration with clinical imaging, using geometries derived from 3D reconstruction of the *LV* without further manipulation other than the congruence of the orifice size.

The numerical solution technique utilizes the Immersed Boundary (*IB*) method (Domenichini, 2008; Fadlun et al., 2000). In this approach the *LV* the geometry is immersed inside the computational domain and the inflow/outflow velocity profiles are automatically ensured by mass conservation from the system of equations (see: Mangual et al., 2012b, Mangual et al., 2012a, for more details). Exemplary end-diastolic geometry for a healthy and *DCM* ventricle are shown in Fig. 1. Previous studies have suggested that *LV* flow is transitional or weakly

Table 1
Summary of clinical characteristics measured for the healthy subjects and *DCM* patients.

	Healthy subjects	DCM patients	P-value
Volunteers	20	8	–
Male	19	6	–
Female	1	2	–
Age [yrs])	18.85 ± 3.54	62.12 ± 16.43	< 0.000001
Heart rate [bpm]	72.20 ± 6.56	72.62 ± 9.47	0.89
EF [%]	55.38 ± 3.52	17.77 ± 6.40	< 0.000001
LV Volume [mL]			
End diastolic	139.73 ± 29.34	239.03 ± 51.56	< 0.000001
End systolic	66.18 ± 18.91	198.51 ± 55.26	< 0.000001
Stroke volume	73.55 ± 13.78	40.51 ± 12.30	0.000003
Mitral valve area [cm^2]	5.36 ± 1.37	6.07 ± 1.07	0.0066
Aortic valve area [cm^2]	3.90 ± 0.47	5.01 ± 0.81	0.000084

DCM: dilated cardiomyopathy; **EF**: ejection fraction; **LV**: left ventricle. Values are presented as mean $\pm$ SD for the volunteers in each group.
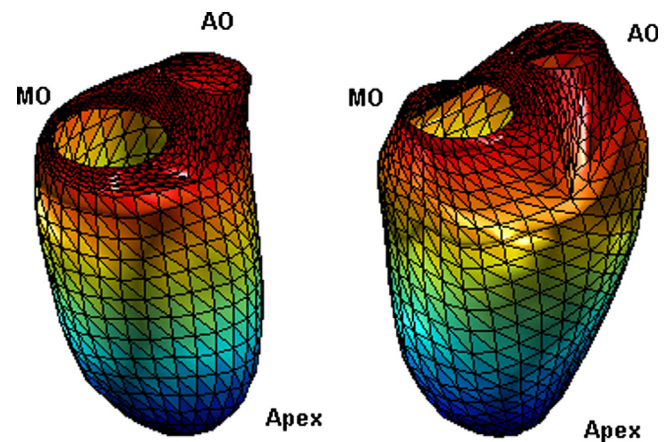

Fig. 1. Exemplar LV geometries at end diastole extracted from 3D echocardiography imaging. Healthy (left, EDV=90 mL) and dilated (right, EDV=175 mL) ventricles. The mitral orifice (MO), aortic orifice (AO) and apex are labeled for reference.

turbulent, leading to small scale eddies (Pierrakos and Vlachos, 2006, Querzoli et al., 2010), yet in our previous work (Mangual et al., 2012a), grid refinement analysis proved that smaller scales are not missed and resolution is adequate. When using *DNS*, lack of sufficient resolution may lead to energy accumulation; careful analysis of the numerical results was done to ensure this was not the case.

2.3. Fluid dynamics analysis

LV fluid dynamic is evaluated by several metrics selected to quantify the flow properties.

Vortex Formation Time (*VFT*): This dimensionless parameter measures the process of vortex formation from the mitral jet. It is the duration of the formation process–until deceleration–normalized with flow time, that would be required to travel the length of one valvular diameter; it represents the length of the jet, normalized with valve diameter. *VFT* is computed as the time integral of the transmitral velocity from end systole (*ES*) to the first diastolic peak, it measures the quality of the vortex formation process and optimum *LV* filling. *VFT* of 4 corresponds to an optimal vortex formation process (Gharib et al., 1998; Kheradvar and Pedrizzetti, 2012). High values are associated with the breakdown of the forming vortex and turbulence, while lower correspond to suboptimal propulsion. Given that the *VFT* is proportional to the *LV* Ejection Fraction (*EF*) (Gharib et al., 2006) the ratio of *VFT/EF* is also analyzed.

Kinetic Energy Dissipation: Calculated from the time integral of the rate of kinetic energy (*KE*) viscous dissipation (Pedrizzetti and Domenichini, 2005; Pedrizzetti et al., 2010) and measures the amount of energy, ΔKE, which is dissipated into heat during the phases of the cycle. Smooth regular flow presents low values of dissipation; whereas high dissipation is associated with a complex flow, possibly turbulent. Absolute dissipation is also influenced by the amount of *KE* inflow into the *LV*, which depends on the Stroke Volume *SV*. In order to build an indicator that is least influenced by this, dissipation is also presented in dimensionless terms after normalization of ΔKE with the flux of *KE* across the mitral orifice,

KE_{inflow}. This index, $\Delta KE/KE_{inflow}$, represents a measure of the actual dissipation occurring within the LV with respect to the originally available energy, an EF-independent parameter.

Flow Transit: A method to evaluate the fluid turnover in the LV can be built on the Residence Time Distribution concept widely employed in chemical engineering (Nauman, 2007). Conceptually, the SV that is ejected during systole is partly made of fresh blood that entered into the LV during the previous diastole, and partly of blood that entered during two (or more) previous diastolic phases and has been retained in the LV for one (or more) heartbeats. In order to quantify the efficiency of the blood turnover in the LV we consider the blood that entered during a first diastole as a virtual tracer, we then evaluate the percentage of that tracer that is ejected after one systole, after the second systole and so on, until the whole tracer has been cleared out of the LV cavity.

This gives a *blood transit curve*, F_n, ($n=1, 2, 3…$), that measures the percentage of SV that has been ejected after a number n of heartbeats. This curve starts from 0 at the end of the initial filling phase (the first ECG R-wave), and asymptotically approaches the unitary value when all the SV has been ejected. The value after one heartbeat, F_1, represents the percentage of the SV ejected during the first systole; the value F_2 is the percentage of the SV that is cleared from the LV after 2 systolic cycles, etc.

From the first, fundamental, value, F_1, it is possible to compute the indicators introduced in the CMR literature (Bolger et al., 2007; Eriksson et al., 2010). In particular, the Direct Flow, $V_{Direct}=F_1 \times EF$, is the percentage of the LV End Diastolic Volume (EDV) that directly flows from inlet to outlet during one heartbeat. The Retained inflow comes from the difference $V_{Retained}=SV-V_{Direct}$, and it is also equal (theoretically) to the Delayed Ejection, $V_{Delayed}=V_{Retained}$, for mass conservation, and the Residual Volume is calculated from the difference $V_{Residual}=ESV-V_{Delayed}$ (see supplemental online figure for a graphical representation of these sub-volumes). The dynamics of the tracer is computed by DNS of the corresponding convection-diffusion equation (Mangual et al., 2012a).

2.4. Statistical analysis

All the data are presented as mean ± standard deviation for each group analyzed. Comparison of the quantities amongst the two groups was performed using Student *T*-test, two-sided p-coefficient was used to determine differential statistical significance. Given the volumetric differences between the two groups, several indicators are expected to be significant; however differential significance is employed to compare the different parameters. A minimum limit is set to $p=10^{-6}$ considered as full significance within this limited sample.

3. Results

3.1. Clinical characteristics

Clinical characteristics are summarized in Table 1. No significant difference was noted in heart rate between the healthy and DCM groups (mean heart rate 72.20 ± 6.56 vs. 72.62 ± 9.47 bpm respectively, $p=0.89$). As expected, EF was highly significant lower in DCM group (17.8 ± 6.4 vs. $55.4 \pm 3.5\%$, $p < 10^{-6}$) and ventricle size was significantly larger in the DCM group (EDV: 240 ± 52 vs. 140 ± 30 ml, $p < 10^{-6}$; ESV: 200 ± 55 vs. 66 ± 19 mL, $p < 10^{-6}$). Despite the larger ventricular size, SV was lower in the DCM group ($p=3 \times 10^{-6}$). The estimated mitral/aortic orifice area used for the simulations showed no significant difference among the groups, although the DCM volunteers resulted in larger orifices on average.

3.2. Phenomenological flow description

Figs. 2 and 3 show the flow field inside the LV during mid-diastole (end of the E-wave) and end diastole (ED), respectively. The pictures on the left side show the flow on a longitudinal plane across the mitral\aortic orifices and the apex, in terms of in-plane velocity vectors and color-coded vorticity (local fluid rotation, red=clockwise, blue=counter-clockwise). Pictures on the central column show the three dimensional vortex pattern (by the λ_2-method, (Jeong and Hussain, 1995)) and the far right column depicts the pressure distribution on 2D longitudinal planes obtained from the simulations with the inset profile corresponding to the base to apex pressure gradient throughout a cardiac cycle.
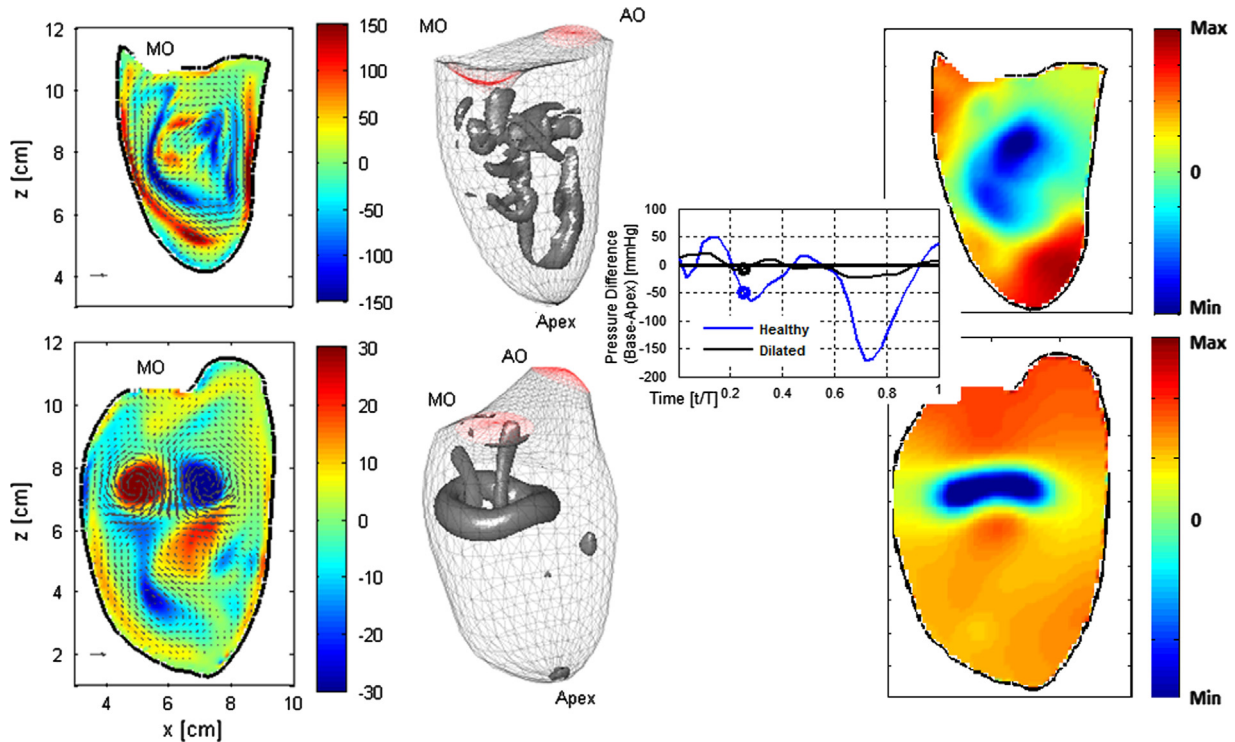

Fig. 2. Diastolic intraventricular flow at the end of the E-wave for one healthy subject (top row, EF=56%) and for a patient with DCM (bottom row, EF=18%); the flow is reported on a longitudinal cross-section on the left (velocity as arrows, unit vector is 50 cm/s, vorticity as color-coded in s^{-1}), and the three-dimensional vortex field on the center (by iso-surface of the λ_2 field, $\lambda_2=-1500$ s^{-2} for the healthy case and -200 s^{-2} for the *DCM* one). Pressure fields are shown on the right column, blue and red color fields correspond to minimum and maximum pressure, respectively. Inset plot corresponds to the base/apex pressure difference throughout a cardiac cycle. The healthy flow shows a counter-clockwise wide rotatory pattern taking most of the cavity, with a three dimensional vortex structure that has elongated toward the apex. In the *DCM* case the formed vortex ring is of lower strength, it remains rather compact in the middle of the cavity.
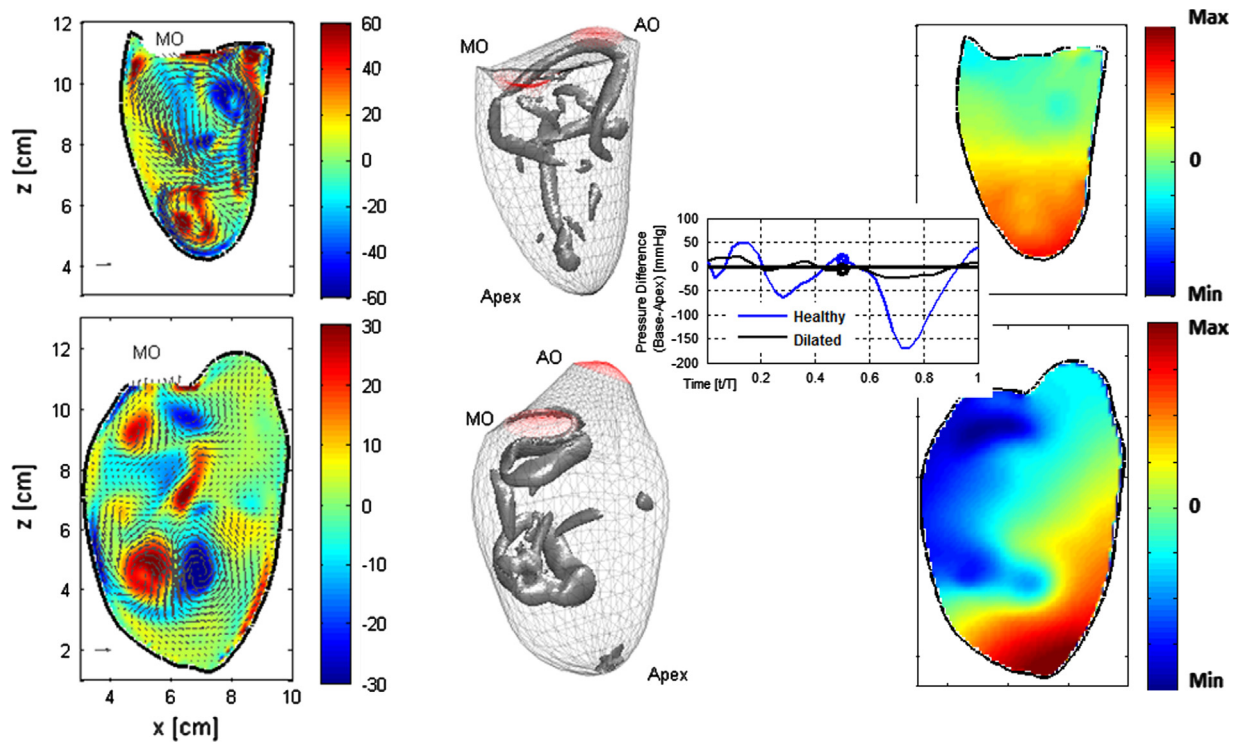
Fig. 3. Diastolic intraventricular flow at the end of the A-wave, before the onset of contraction, for one healthy subject (top row, EF=56%) and for a patient with *DCM* (bottom row, EF=18%); the flow is reported on a longitudinal cross-section on the left (velocity as arrows, unit vector is 50 cm/s, vorticity as color-coded in s^{-1}), and the three-dimensional vortex field on the right (by iso-surface of the λ_2 field, $\lambda_2 = -1500$ s^{-2} for the healthy case and -200 s^{-2} for the DCM one). Pressure fields are shown on the right column, blue and red color fields correspond to minimum and maximum pressure. Inset plot corresponds to the base/apex pressure difference throughout a cardiac cycle. The normal end-diastolic flow is made of a main circulatory pattern with flow directed toward the *LV* outflow tract; it is due to the vortices formed during the E- and A-waves that can still be recognized in the three-dimensional view. Differently, the *DCM* patient shows two compact rings in the center of the cavity inducing a local circulation only. (For interpretation of the references to color in this figure, the reader is referred to the web version of this article.)

In the healthy ventricle (EF=56%) mid-diastolic flow (Fig. 2) was characterized by a predominant counter-clockwise pattern that covers the entirety of the central cavity; the 3D view shows an elongated vortex structure coming from the stretching of an initially ring-shaped vortex. In *DCM* (EF=18%) the vortex formation produces a ring of lower strength that remains coherent in the middle of the cavity. End-diastolic flow (Fig. 3) in the healthy subject revealed a main circulatory pattern with flow directed toward the *LV* outflow tract. Circulation is due to the merged action of the vortices formed during the E- and A-waves, while the individual cores of the two vortices can be well recognized in the three-dimensional view. In contrast, the *DCM* patient showed that the vortex wake formed during diastole maintains its compactness solely in the center of the cavity, inducing only local circulation. Pressure fields on the right hand columns of Figs. 2 and 3 coincide with the main vortex structure inside the *LV* chamber, where low pressure regions correspond to the location of the vortex cores.

3.3. Quantitative flow analysis

Results on the flow parameters are summarized in Table 2. The *VFT* for the healthy group was 4.33 ± 0.37, *DCM* patients exhibited a significantly lower value of *VFT* around 1.5 ($p < 10^{-6}$). The ratio between *VFT* and *EF* was non-significantly different between the two groups ($p=0.16$).

The total *KE* dissipation, ΔKE, for the healthy and *DCM* groups is reported during diastole, systole, and the whole heartbeat. *KE* dissipation in the healthy subjects were greater during filling than during contraction. Alternatively, the *DCM* group had an almost constant rate of dissipation during the whole heartbeat with smaller values over all periods ($p=10^{-5}$, during diastole; $p < 10^{-6}$ for systole). It must be stated that the *DCM* group had a total amount of

Table 2
Summary of *LV* flow properties measured for the healthy subjects and *DCM* patients.

	Healthy subjects	DCM patients	P-value
Vortex formation time, *VFT* [–]	4.33 ± 0.37	1.49 ± 0.53	< 0.000001
VFT/EF ratio [–]	7.85 ± 0.79	9.03 ± 3.13	0.16
KE Dissipation ΔKE [mJ]	0.2270 ± 0.08	0.0246 ± 0.01	< 0.000001
Diastolic	0.1739 ± 0.07	0.0127 ± 0.01	0.000001
Systolic	0.0531 ± 0.02	0.0119 ± 0.01	< 0.000001
KE Inflow KE_{inflow} [mJ]	14.80 ± 4.90	1.22 ± 0.61	< 0.000001
KE Dissipation index	1.52 ± 0.25	2.05 ± 0.26	0.00007
$\Delta KE/KE_{inflow}$ [%]			
Diastolic	1.15 ± 0.22	1.04 ± 0.22	0.29
Systolic	0.37 ± 0.11	1.01 ± 0.17	< 0.000001
Transit curve [% of *SV*]			
1 heartbeat	48.66 ± 4.73	3.78 ± 2.52	< 0.000001
2 heartbeats	80.02 ± 3.86	21.81 ± 14.12	< 0.000001
4 heartbeats	98.03 ± 1.88	53.92 ± 20.33	< 0.000001
8 heartbeats	100.00 ± 0.00	86.27 ± 9.39	0.000005
Flow paths [% of *EDV*]			
Direct flow	25.69 ± 3.99	0.69 ± 0.49	< 0.000001
Delayed flow	26.44 ± 1.56	16.56 ± 5.30	< 0.000001
Retained inflow	26.44 ± 1.56	16.56 ± 5.30	< 0.000001
Residual flow	21.43 ± 3.52	66.19 ± 10.90	< 0.000001

DCM: dilated cardiomyopathy; **VFT**: vortex formation time; **EF**: ejection fraction; **KE**: kinetic energy; **EDV**: end diastolic volume; **SV**: stroke volume. Values are presented as mean $\pm$ SD for the volunteers in each group.

dissipation that, on average, was about one order of magnitude lower than that of the healthy subjects, being strictly related to the lower level of *KE* available from the inflow ($p < 10^{-6}$). After normalization, the *KE* dissipation index, $\Delta KE/KE_{inflow}$, was numerically comparable in the two groups, with no significant difference during
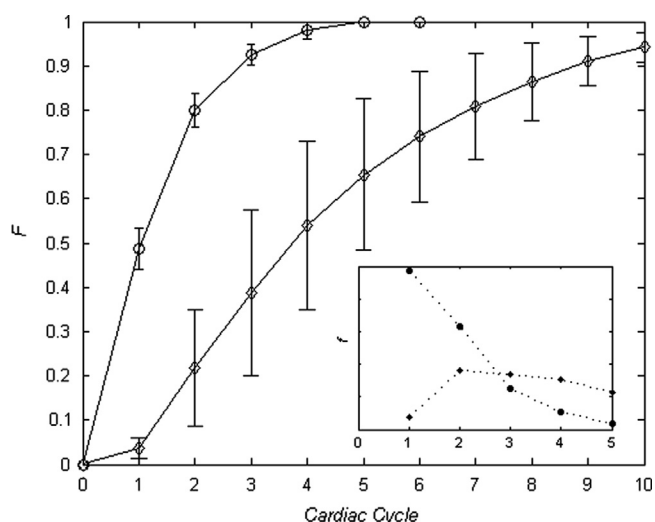
Fig. 4. Blood transit curve: average curve from the healthy (circles) and the pathologic *DCM* subjects (diamonds). Inset depicts the beat-by-beat differences. The normal transit curve shows a fairly homogeneous behavior with about 50% of the flow entered during diastole ejected during the following systole, and over 90% of it after 3 beats. In the *DCM* patients, variability is larger, however only a minimal percentage of blood transits within few beats, and a 90% renewal is reached only after about 10 beats.

diastole ($p=0.29$) but a significant lower dissipation ($p < 10^{-6}$) persisting during systole.

The blood transit curves for the healthy and the *DCM* volunteers are plotted in Fig. 4 (circles for healthy and diamonds for *DCM* cases) in terms of mean and standard deviation. In the healthy group the curve reaches a value of $F_1 = 48 \pm 5\%$ after the first systole and saturates (100%) after 4 beats. The *DCM* group exhibits a broader variability in the transit curve with values significantly lower. After one beat the *DCM* curve is lower than 4% ($p < 10^{-6}$). The difference remains large in the two groups after 2, 4, 8 beats, ($p < 10^{-6}$, $< 10^{-6}$, 5×10^{-6}). Other values that can be constructed from the transit curve (time to 50%, time to 75%, etc.), are not reported to avoid redundant figures. The direct flow, $F_1 \times EF$, corresponds to 26% and 1% of *EDV* in healthy subjects and *DCM*. The dilated ventricles exhibited a much lower delayed and retained flow ($p < 10^{-6}$) and a significantly higher residual flow of 66% vs. 21% in healthy vs. dilated ventricles ($p < 10^{-6}$).

4. Discussion

4.1. Technical aspects

Combination of recent 3D echocardiography and numerical techniques provide an evaluation of *LV* flow that is alternative and complementary to other existing solutions. Other techniques available for *LV* flow assessment are the Echo Doppler, Echo-*PIV* (Particle Image Velocimetry), and phase-contrast *CMR* (Sengupta et al., 2012b). These have the advantage of being direct in-vivo measures without requiring reconstruction methods, although each presents limitations. Doppler is constrained to one component of the velocity vector and cannot be used for the assessment of flows with varying direction. Echo-*PIV*, which has the advantage of acquiring high frame rate is still limited to two-dimensional analysis, has low spatial resolution and moderate accuracy (Sengupta et al., 2012b). Recent developments are also in progress for multi-planar and 3D imaging (Sengupta et al., 2012a), although quality may be reduced further. *CMR* is the only technique that permits three-dimensional acquisitions with good quality and some limitations in temporal and spatial resolution. The resulting flow is averaged over a large number of heartbeats, masking high frequency fluctuations (small vortices) and beat-by-beat variability.

The approach presented here suffers from low temporal resolution, due to the low frame rate of 3D echocardiography, and reduced spatial accuracy, because although it theoretically produces a fully spatially resolved 3D flow fields, the effective flow details are dependent on those of the reconstructed geometry that are only approximate. In other words, *DNS* is acknowledged as theoretically exact and its effective accuracy simply reflects the accuracy of the original input information provided by imaging. Therefore this approach provides the intra *LV* blood motion with a temporal accuracy of 3D echocardiography, limited to gross features of *LV* flow patterns neglecting details due to smaller elements (trabeculae, chordae tendineae) not present in the imaging. Nevertheless, this method is noninvasive and can be performed with relative ease from post-processing without additional imaging costs.

4.2. Energetic flow aspects

The present study provides novel insights about pathologic alterations in *LV* fluid dynamics. The phenomenological organization of the *LV* flow in the normal subjects is in agreement with those reported in the literature. It has been confirmed that normal diastolic filling is characterized by the presence of a 3D vorticity structure that develops into a dominant asymmetric vortex, a relatively smooth wheel-like motion over the whole cavity, which is associated with flow redirection toward the aorta (Kilner et al., 2000; Pedrizzetti and Domenichini, 2005). This global picture significantly changes in the context of *DCM*. The reduced cardiac function reflects weakening of the diastolic mitral jet which penetrates less deeply into the wider *LV*, with a small vortex in the center of the cavity as shown in previous models (Baccani et al., 2002), that does not support flow redirection toward the outflow. Intraventricular pressure gradients are primarily given by the time derivative of the velocity (thus it presents two acceleration/deceleartion peaks for every velocity peak). Preliminary high frame rate (200 Hz) in vivo evaluations show peaks even during the isovolumic phases, not accessible in our relatively low time resolution model (following that of 3D echo, as discussed). We cannot enter here in depth in this interesting, in-progress subject; however we reported the time-varying profile of the base-apex pressure difference, as requested, that shows a reduction of IVPG in DCM (related to reduction of transvalvular flow).

Healthy *VFT* range very much agrees with the theoretical optimal value (Gharib et al., 2006), while the pathological low *VFT* means that the jet is weak and does not deeply penetrate the *LV*. Similarly the low values of the *KE* dissipation confirm that the flow is not vigorous. However, all these indicators are directly influenced by the *EF*. In fact, the *VFT* can be computed in a way where the direct proportionality with the *EF* is explicit (Gharib et al., 2006) and the correlation between *EF* and *VFT* has been previously reported in clinical study (Nucifora et al., 2010). In fact, the ratio *VFT/EF*, which removes the influence of *EF* on the *VFT* value, presents a non-significant difference between the two groups, meaning that *VFT* does not provide information incremental to *EF* in this specific clinical context. These results are similar to those recently reported by Stewart et al. (Stewart et al., 2012), in which the *VFT* was shown not to weigh on overall cardiac function, but in fact just a sign of optimal *LV* filling.

The dimensional *KE* dissipation is also dependent on the amount of *KE* injected in the chamber and thus on the *SV*. Previous works dealing with dissipation compared cases with the same *EF* and *SV* (Pedrizzetti and Domenichini, 2005; Pedrizzetti et al., 2010). Therefore, it is necessary to verify whether this indicator brings information that is incremental to *LV* volumetric measures. To this purpose, the dimensionless dissipation index is an energetic indicator that is

conceptually independent from *EF* or *SV*. During diastole it is comparable between healthy and *DCM* subjects, meaning that the filling is accompanied by the loss of a similar percentage of the incoming *KE*; however, the systolic ejection is associated with a significantly higher relative *KE* dissipation in *DCM*. This can be explained by the absence of the typical redirection of flow toward the *LV* outflow tract in *DCM*, with the requirement of additional work to deviate toward the aorta the quiescent or incorrectly moving fluid.

4.3. Flow transit aspects

The concept of the blood transit curve gives a synthesis of the flow properties in terms of blood turnover inside the *LV* that can be useful for defining the quality of flow passage through the *LV* and the presence of stagnation. This curve represents an extension of the previously introduced subdivision of the *EDV* into 4 sub-volumes (Bolger et al., 2007; Eriksson et al., 2010) that can be recovered from the first value of the blood transit curve in combination with the *ED* and *ES* volumes. The flow in *DCM* presents a significantly slower renovation of the blood contained in the *LV*, this is witnessed by the significantly reduction of the direct flow and an increase of either the delayed or the residual volumes. This difference was previously reported in *CMR* literature (Carlhäll and Bolger, 2010), although in quantitative terms the *CMR* literature present higher direct flow values (Eriksson et al., 2010) and changes in the other dependent sub-volumes. Such an inter-technology variability can be justified on one side by the regularity in *CMR* flow that, averaged over several heartbeats, does not include higher frequency that mix the fluid and reduce coherence in the transit flow.

The transit curve was built in a way to be independent from *SV* or *EF* and, in principle, purely characterizing fluid mechanics properties that are additive to volumetric measures. The curve values are all largely reduced in *DCM* patients characterizing the longer time of blood residence and stagnation in the *LV*. Besides the individual values, the time profile of the transit curve represents a synthetic description of the *LV* wash-out process.

4.4. Clinical aspects

Blood flow in the *LV* shows the formation of vortices accompanying the smooth redirection of the mitral flow to the outflow track. Vortices are crucial elements of fluid motion and essential to the dynamic equilibrium between the hyperelastic tissues and the spatial distribution of time-varying blood pressure and shear stress (Sengupta et al., 2012b). Such a natural balance is largely corrupted in patients that undergo remodeling and appears restored in stable asymptomatic patients (Carlhäll and Bolger, 2010; Kheradvar et al., 2012; Nucifora et al., 2010). Moreover, cardiac flow is immediately (meaning "within a single heartbeat") affected by small changes in the surrounding conditions. Therefore blood flow is a natural early indicator of progressive alterations in cardiac function. Although it is a common belief that fluid dynamics actively participate in the progression of cardiac inefficiency and remodeling (Yang et al., 2007), the role of *LV* flow in remodeling has not been investigated.

Diagnostic markers based on flow were applied to *DCM* pathology, that is largely detectable by a number of existing clinical indicators, without the need of fluid dynamics or sophisticated technologies. Nevertheless, this was a necessary first step, in clear clinical conditions, for the development of clinical markers that are intrinsically flow-based and that, in perspective, could be useful in discriminating quantitatively diseases and differentiate severity of same diseases.

Parameters that are pure descriptors of cardiac fluid dynamics, cleared from the influence of volumetric changes, may contain information that is additive and integrative to measures based on myocardial mechanics. Given that flow is immediately affected by minor changes in the surrounding conditions, it is conceivable that flow may be supportive for the early diagnosis of progressive *LV* dysfunction before evident irreversible modifications in tissues have been developed.

5. Limitations

The first limitation of the study is related to the small size of the populations. Nevertheless, the high differentiation between the two groups and the significant statistical differences mitigated this limiting aspect. On the opposite perspective, a major limitation is given by the large difference between the two groups. Although this was nearly unavoidable for building initial references, this fact does not ensure that the results obtained here can be useful to evidence minor differences during early stages of pathology.

From a more technical point of view, the simulations do not include dynamic information about the valve dynamics nor atrial geometry that influences specific features of the entry jet. Details of the endocardial geometry with trabeculae may also influence intraventricular flow; and limitations of the frame rate, dictated by echocardiography, do not allow accurate resolution, thus hiding details such as in the isovolumic phases. For these reasons we mainly focused on parameters based on properties integrated over the whole *LV* volume and over the whole heartbeat cycles to avoid variability due to inaccurate spatial description or low time resolution.

6. Conclusions

This pilot study on pathological changes in *LV* blood motion demonstrated the feasibility and diagnostic building support given by the combination of medical imaging with numerical solutions. The comparative analysis of two well different groups of healthy and *DCM* subjects evidenced the reduction of energetic efficiency and the increase of flow stagnation that accompany pathologic blood streaming. The building of purely fluid dynamics indicators facilitates the clinical exploitation of blood flow because these might be well integrative to existing ones describing myocardial mechanics. These initial results, jointly with the potential predictive ability of fluid mechanics, open a possible new perspective in early diagnosis of progressive diseases.

7. Conflict of interest

None.

Acknowledgments

Appendix A. Supporting information

Supplementary data associated with this article can be found in the online version at http://dx.doi.org/10.1016/j.jbiomech.2013.04.012.

References

Baccani, B., Domenichini, F., Pedrizzetti, G., Tonti, G., 2002. Fluid dynamics of the left ventricular filling in dilated cardiomyopathy. Journal of Biomechanics 35, 665–671.

Bolger, A.F., Heiberg, E., Karlsson, M., Wigstrom, L., Engvall, J., et al., 2007. Transit of blood flow through the human left ventricle mapped by cardiovascular magnetic resonance. Journal of Cardiovascular Magnetic Resonance 9, 741–747.

Carlhäll, C.J., Bolger, A.F., 2010. Passing strange. Circulation: Heart Failure 3, 326–331.

Cimino, S., Pedrizzetti, G., Tonti, G., Canali, E., Petronilli, V., et al., 2012. In vivo analysis of intraventricular fluid dynamics in healthy hearts. European Journal of Mechanics —B/Fluids 35, 40–46.

De Luca, A., Stefani, L., Pedrizzetti, G., Pedri, S., Galanti, G., 2011. The effect of exercise training on left ventricular function in young elite athletes. Cardiovasc Ultrasound 9, 27.

Dimasi, A., Cattarinuzzi, E., Stevanella, M., Conti, C.A., Votta, E., Maffessanti, F., Ingels, N.B., Redaelli, A., 2012. Influence of mitral valve anterior leaflet in vivo shape on left ventricular ejection. Cardiovascular Engineering and Technology 3, 388–401.

Domenichini, F., 2008. On the consistency of the direct forcing method in fractional step solutionof the Navier-Stokes equation. Journal Computational Physics 227, 6372–6384.

Eriksson, J., Carlhall, C., Dyverfeldt, P, Engvall, J., Bolger, A., Ebbers, T., 2010. Semi-automatic quantification of 4D left ventricular blood flow. Journal of Cardio-vascular Magnetic Resonance 12, 9.

Fadlun, E.A., Verzicco, R., Orlandi, P., Mohd-Yusof, J., 2000. Combined immersed-boundary finite-difference methods for three-dimensional complex Flow simulations. Journal of Computational Physics 161, 35–60.

Gharib, M., Rambod, E., Kheradvar, A., Sahn, D.J., Dabiri, J.O., 2006. Optimal vortex formation as an index of cardiac health. Proceedings of the National Academy of Sciences 103, 6305–6308.

Gharib, M., Rambod, E., Shariff, K., 1998. A universal time scale for vortex ring formation. Journal of Fluid Mechanics 360, 121–140.

Jeong, J., Hussain, F., 1995. On the identification of a vortex. Journal of Fluid Mechanics 285, 69–94.

Kheradvar, A., Assadi, R., Falahatpisheh, A., Sengupta, P.P., 2012. Assessment of transmitral vortex formation in patients with diastolic dysfunction. Journal of American Society of Echocardiography 25, 220–227.

Kheradvar, A., Pedrizzetti, G., 2012. Vortex Formation in the Cardiovascular System. Springer-Verlag, London164.

Kilner, P.J., Yang, G.Z., Wilkes, A.J., Mohiaddin, R.H., Firmin, D.N., Yacoub, M.H., 2000. Asymmetric redirection of flow through the heart. Nature 404, 759–761.

Lancellotti, P., Moura, L., Pierard, L.A., Agricola, E., Popescu, B.A., Tribouilloy, C., Hagendorff, A., Monin, J.L., Badano, L., Zamorano, J.L., 2010. European Associa-tion of Echocardiography recommendations for the assessment of valvular regurgitation. Part 2: mitral and tricuspid regurgitation (native valve disease). European Journal of Echocardiography 11, 307–332.

Mangual, J.O., Domenichini, F., Pedrizzetti, G., 2012a. Describing the highly three dimensional right ventricle flow. Annual Review of Biomedical Engineering 40, 1790–1801.

Mangual, J.O., Domenichini, F., Pedrizzetti, G., 2012b. Three dimensional numerical assessment of the right ventricular flow using 4D echocardiography boundary data. European Journal of Mechanics —B/Fluids 35, 25–30.

Mihl, C., Dassen, W., Kuipers, H., 2008. Cardiac remodelling: concentric versus eccentric hypertrophy in strength and endurance athletes. Netherlands Heart Journal 16, 129–133.

Nauman, E.B., 2007. Residence Time Distributions. In Chemical Reactor Design, Optimization, and Scaleup. John Wiley & Sons, Inc.535–574.

Nijveldt, R., Hofman, M.B., Hirsch, A., Beek, A.M., Umans, V.A., et al., 2009. Assessment of microvascular obstruction and prediction of short-term remo-deling after acute myocardial infarction: cardiac MR imaging study. Radiology 250, 363–370.

Nucifora, G., Delgado, V., Bertini, M., Marsan, N.A., Van de Veire, N.R., et al., 2010. Left ventricular muscle and fluid mechanics in acute myocardial infarction. Journal of American Cardiology 106, 1404–1409.

Pedrizzetti, G., Domenichini, F., 2005. Nature optimizes the swirling flow in the human left ventricle. Physical Review Letters 95, 108101.

Pedrizzetti, G., Domenichini, F., Tonti, G., 2010. On the left ventricular vortex reversal after mitral valve replacement. Annual Review of Biomedical Engineer-ing 38, 769–773.

Pierrakos, O., Vlachos, P.P., 2006. The effect of vortex formation on the left ventricular filling and mitral valve efficiency. Journal of Biomechical Engineer-ing 128, 527–539.

Querzoli, G., Fortini, S., Cenedese, A., 2010. Effect of the prosthetic mitral valve on vortex dynamics and turbulence of the left ventricular flow. Physics of Fluids 22, 041901.

Sengupta, P.P., Narula, J., 2008. Reclassifying heart failure: predominantly sub-endocardial, subepicardial, and transmural. Heart Fail Clinics 4, 379–382.

Sengupta, P.P., Pedrizzetti, G., Narula, J., 2012a. Multiplanar visualization of blood flow using echocardiographic particle imaging velocimetry. JACC Cardiovasc Imaging 5, 566–569.

Sengupta, P.P., Pedrizzetti, G., Kilner, P.J., Kheradvar, A., Ebbers, T., et al., 2012b. Emerging Trends in CV Flow Visualization. JACC Cardiovascular Imaging 5, 305–316.

Stewart, K.C., Charonko, J.C., Niebel, C.L., Little, W.C., Vlachos, PP., 2012. Left ventricular vortex formation is unaffected by diastolic impairment. American Journal of Physiology—Heart Circulatory Physiology 303, H1255–H1262.

Veronesi, F., Corsi, C., Sugeng, L., Mor-Avi, V., Caiani, E.G., Weinert, L., Lamberti, C., Lang, R.M., 2009. tudy of A sfunctional anatomy of aortic-mitral valve coupling using 3D matrix transesophageal Echocardiography. Circulation Cardiovascular Imaging 2, 24–31.

Wu, E., Ortiz, J.T., Tejedor, P., Lee, D.C., Bucciarelli-Ducci, C., et al., 2008. Infarct size by contrast enhanced cardiac magnetic resonance is a stronger predictor of outcomes than left ventricular ejection fraction or end-systolic volume index: prospective cohort study. Heart 94, 730–736.

Yang, G.-Z., Merrifield, R., Masood, S., Kilner, P.J., 2007. Flow and myocardial interaction: an imaging perspective. Philosophical Transactions of the Royal Society B 362, 1329–1341.